ICMIEE22-163

Unsteady Convection and Mass Transport over a Stretching Sheet in a Saturated Porous Medium with Magnetic Field

Mahamudul Hassan Milon[1], Md. Hasanuzzaman[2,] and Akio Miyara[3, 4]*

[1]Department of Computer Science and Engineering, North Western University, Khulna-9100, Bangladesh
[2]Department of Mathematics, Khulna University of Engineering & Technology, Khulna-9203, Bangladesh
[3]Department of Mechanical Engineering, Saga University, Saga-shi, 840-8502, Japan
[4]International Institute for Carbon-Neutral Energy Research, Kyushu University, Fukuoka-shi, 819-0395, Japan

ABSTRACT

An analysis of a time-dependent magneto-convective heat-mass transport upon a stretching sheet in a saturated permeable medium with the magnetic field are discussed. The governing partial differential equations (PDEs) are transformed into ordinary differential equations (ODEs) by imposing the similarity transformation. The transformed governing ODEs are solved numerically using finite difference method by shooting technique in ODE45 MATLAB software. The numerical results are shown graphically and tabular form performing the impacts of several non-dimensional parameters/numbers entering into the current problem. With an increase in the values of the Darcy number and magnetic force parameter reduction in the fluid velocity. The concentration and the temperature of the fluid decrease for moving values of the Schmidt number and the Prandtl number, respectively. The mass transfer rate increases by about 46%, due to increasing the Schmidt number (0.5-1.0). The heat transfer rate increases by about 22% due to improving the Prandtl number (0.71-1.0). The local skin-friction coefficient decreases by about 24% and 21% due to improving the magnetic force parameter (1.5-3.0) and Darcy number (0.6-1.6), respectively.

Keywords: MHD, heat and mass transfer, stretching surface, permeable medium.

1. Introduction

The phenomenon of MHD free heat transfer and mass transfer on an embedded vertical permeable sheet has attracted the interest of many research scholars due to its various applications in technology and science. The free convection of mass transfer of viscous fluid passing upon a permeable medium has been studied by Yamato et al. [1]. The combined natural and forced convection flow about an inclined surface in a permeable medium has been explained by Cheng [2]. The effect of heat and mass transfer upon MHD unsteady convection flow through an inclined plate by using the finite difference method has been analyzed by Kumar et al [3]. Gupta and Gupta [4] examined the effect of the suction or blowing on heat and mass transfer above a stretching plate. The effects of a magnetic field and thermocapillary on a time-dependent elastic stretching sheet in a thin liquid film have been discussed by Noor and Hashim [5]. Using the homotopy analysis method, Wang and Pop [6] presented a solution to the unsteady stretching flow problem in the case of finite thickness. The influence of thermal radiation on a time-dependent convective heat transfer flow through a stretching sheet in a saturated permeable medium has been investigated by Khader and Megahed [7]. In their simulation, they solved the resulting system of algebraic equations by using the finite difference method. Also, Khader and Megahed [7] considered only energy and momentum equations. Hasanuzzaman et al [8] extended Khader and Megahed [7] problems by considering energy, concentration, and momentum equations. They also applied the shooting technique to solve the non-linear ODEs. Now, we extended Hasanuzzaman et al [8] by considering the magnetic force term.

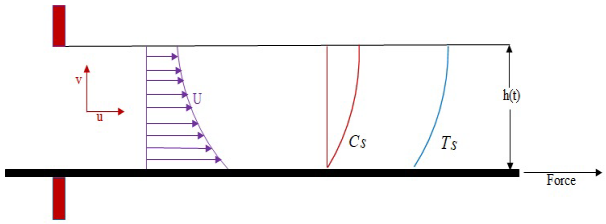

The outcome of this study is to estimate a time-dependent magneto-convective heat-mass transport upon a stretching sheet in a saturated porous medium. The current research is to extend the works of Hasanuzzaman et al [8] by considering the effects of the magnetic force parameter. The impacts of the thermo-physical parameters on the flow and heat-mass transport characteristics are discussed in detail. Additionally, tabular forms are shown the effects of nin-dimensional parameters or numbers on the Nusselt number, Sherwood number, and local skin friction coefficient.

2. Governing Equations

Let us consider a time-dependent Newtonian fluid flow in a thin liquid film upon a stretching surface including a magnetic force. Figure 1 shows the physical model and coordinate systems. The continuous surface has a velocity profile *U(x, t)* and temperature and concentration distributions are $T_s(x,t)$ and $C_s(x,t)$, respectively in its plane parallel to the x-axis at y = 0. A uniform thin liquid film thickness $h(t)$ lies on the horizontal surface.

* Corresponding author. Tel.: +88-01714838750
E-mail addresses: hasanuzzaman@math.kuet.ac.bd

The governing equations for the present problem are given by

The continuity equation-

$$\frac{\partial u}{\partial x}+\frac{\partial v}{\partial y}=0 \tag{1}$$

The momentum equation-

$$\frac{\partial u}{\partial t}+u\frac{\partial u}{\partial x}+v\frac{\partial u}{\partial y}=\frac{\mu}{\rho}\frac{\partial^2 u}{\partial y^2}-\frac{\mu}{\rho K}u-\frac{\sigma' {B_0}^2 u}{\rho} \tag{2}$$

The energy conservation equation-

$$\frac{\partial T}{\partial t}+u\frac{\partial T}{\partial x}+v\frac{\partial T}{\partial y}=\alpha\frac{\partial^2 T}{\partial y^2} \tag{3}$$

The concentration equation-

$$\frac{\partial C}{\partial t}+u\frac{\partial C}{\partial x}+v\frac{\partial C}{\partial y}=D^*\frac{\partial^2 C}{\partial y^2} \tag{4}$$

where the velocity components along the x-axis and y-axis are u and v, respectively. B is the magnetic field, μ is the fluid viscosity, ρ is the fluid density, K is the permeability of the permeable medium surface, C is the fluid concentration, T is the fluid temperature, t is the time, α is the thermal conductivity, C_p is the specific heat at constant pressure, and D^* is the coefficient of mass diffusion.

The boundary conditions for this problem are given by

$$u=U, T=T_s, v=0, C=C_s \text{ at } y=0 \tag{5}$$

$$\frac{\partial T}{\partial y}=\frac{\partial u}{\partial y}=\frac{\partial C}{\partial y}=0, v=\frac{dh}{dt} \text{ at } y=0 \tag{6}$$

where U is the surface velocity at $y=0$. The liquid film thickness is h. The plate continually goes with the velocity U in the $x-$ direction is given by

$$U=\frac{bx}{1-at} \tag{7}$$

where the positive constants a are and b with dimension $(time)^{-1}$.

The forms of the surface temperature, T_s and concentration, C_s of the stretching plate, vary with the distance x and time t given by

$$T_s=T_0-T_{ref}\left(\frac{b\rho x^2}{2\mu}\right)(1-at)^{-\frac{3}{2}} \tag{8}$$

$$C_s=C_0-C_{ref}\left(\frac{b\rho x^2}{2\mu}\right)(1-at)^{-\frac{3}{2}} \tag{9}$$

where C_{ref} and T_{ref} are the constant reference concentration and temperature, respectively and C_0 and T_0 are the concentration and temperature, respectively at the slit for all $t<\frac{1}{a}$.

Now, upon introduce the similarity transformations:

$$\eta=\left(\frac{b\rho}{\mu}\right)^{\frac{1}{2}}(1-at)^{-\frac{1}{2}}\beta^{-1}y \tag{10}$$

$$u=bx(1-at)^{-1}f_\eta(\eta) \tag{11}$$

$$v=-\left(\frac{b\mu}{\rho}\right)^{\frac{1}{2}}(1-at)^{-\frac{1}{2}}\beta f_\eta \tag{12}$$

$$T=T_0-T_{ref}\left(\frac{b\rho x^2}{2\mu}\right)(1-at)^{-\frac{3}{2}}\theta(\eta) \tag{13}$$

$$C=C_0-C_{ref}\left(\frac{b\rho x^2}{2\mu}\right)(1-at)^{-\frac{3}{2}}\phi(\eta) \tag{14}$$

Now, the dimensionless thin film thickness is β. This film thickness is introduced by Noor and Hashim [5].

$$\beta=\left(\frac{b\rho}{\mu}\right)^{\frac{1}{2}}(1-at)^{-\frac{1}{2}}h(t) \tag{15}$$

Using the equations from (7) to (15), the equations $(1)-(4)$ become

$$f'''(\eta)+\gamma\left[\begin{matrix}f(\eta)f'(\eta)-\frac{s}{2}\eta f''(\eta)-\{f'(\eta)\}^2-\\(S+Da)f'(\eta)-Mf(\eta)\end{matrix}\right]=0 \tag{16}$$

$$\theta''(\eta)+\gamma\,\mathrm{Pr}\left[\begin{matrix}f(\eta)\theta'(\eta)-\frac{3}{2}S\theta(\eta)-\frac{S}{2}\eta\theta'(\eta)-\\2f'(\eta)\theta(\eta)\end{matrix}\right]=0 \tag{17}$$

$$\phi''(\eta)+\gamma\,Sc\left[\begin{matrix}f(\eta)\phi'(\eta)-\frac{3}{2}S\phi(\eta)\\-\frac{S}{2}\eta\phi'(\eta)-2f'(\eta)\phi'(\eta)\end{matrix}\right]=0 \tag{18}$$

The transformed boundary conditions are given by:

$$f(0)=0, f_\eta(0)=1, \theta(0)=1, \phi(0)=1 \tag{19}$$

$$f''(1)=0, \theta'(1)=0, \phi'(1)=0, f(1)=\frac{S}{2} \tag{20}$$

where $S=\frac{a}{b}$ is the unsteadiness parameter, $\mathrm{Pr}=\frac{\mu C_p}{k}$ is the Prandtl number, $\gamma=\beta^2$ is the dimensionless film thickness, $Da=\frac{\mu(1-at)}{\rho bk}$ is the Darcy number and the Magnetic force parameter is $M=\frac{\sigma' {B_0}^2\sigma^2}{\rho\upsilon}$.

3. Physical Parameters

The physical parameters for this present problem are given by:

$$C_f=\frac{2}{\beta}f''(0)\mathrm{Re}_x^{-\frac{1}{2}}, Nu_x=\frac{1}{2\beta(1-at)}\theta'(0)\mathrm{Re}_x^{\frac{3}{2}}$$

$$Sh_x=\frac{1}{2\beta(1-at)}\phi'(0)\mathrm{Re}_x^{\frac{3}{2}}$$

where C_f is the local skin-friction coefficient, Nu_x is the local Nusselt number, Sh_x is the local Sherwood number and $\mathrm{Re}_x = \frac{\rho U_x}{\mu}$ is the local Reynolds number.

4. Numerical Analysis

The main purpose of this research is to use the FDM (Finite Difference Methods) for solving the couple ODEs $(16)-(18)$ associated with the boundary conditions $(19)-(20)$. This type of method is examined for efficiency and accuracy in solving different problems (Ali et al. [9] and Cheng and Liu [10]. The domain location of the solution is discretized into FDMs (Finite Difference Methods). The systems of equations $(16)-(18)$ can be rewritten by using the transformation $f'(\eta) = v(\eta)$ in the form

$$f'(\eta) - v(\eta) = 0 \qquad (21)$$

$$v''(\eta) + \gamma \begin{bmatrix} f(\eta)v'(\eta) - \frac{s}{2}\eta\, v'(\eta) - \{v(\eta)\}^2 - \\ (S + Da)\, v(\eta) - M\, f(\eta) \end{bmatrix} = 0 \qquad (22)$$

$$\theta''(\eta) + \gamma \,\mathrm{Pr} \begin{bmatrix} f(\eta)\,\theta'(\eta) - \frac{3}{2}S\theta(\eta) - \frac{S}{2}\eta\,\theta'(\eta) - \\ 2\, v(\eta)\theta(\eta) \end{bmatrix} = 0 \qquad (23)$$

$$\phi''(\eta) + \gamma\, Sc \begin{bmatrix} f(\eta)\phi'(\eta) - \frac{3}{2}S\phi(\eta) \\ -\frac{S}{2}\eta\phi'(\eta) - 2\, v(\eta)\phi(\eta) \end{bmatrix} = 0 \qquad (24)$$

subject to the boundary conditions:

$$f(0) = 0, v(0) = 1, \theta(0) = 1, \phi(0) = 1 \qquad (25)$$

$$v'(1) = 0, \theta'(1) = 0, \phi'(1) = 0, f(1) = \frac{S}{2} \qquad (26)$$

Let us consider the grid size in $\eta-$ direction is $\Delta\eta = h \rangle 0, \Delta\eta = \frac{1}{N}$, with $\eta_i = ih$ for $i = 0,1,.....,N$.

Define $f_i = f(\eta_i)$, $\theta_i = \theta(\eta_i)$ and $\phi_i = \phi(\eta_i)$.

Let the numerical values of f, θ and ϕ are F_i, θ_i and ϕ_i at the $i-th$ node respectively. We take:

$$f'|_i = \frac{f_{i+1} - f_{i-1}}{2h},\ v'|_i = \frac{v_{i+1} - v_{i-1}}{2h}$$

$$\theta'|_i = \frac{\theta_{i+1} - \theta_{i-1}}{2h},\ \phi'|_i = \frac{\phi_{i+1} - \phi_{i-1}}{2h} \qquad (27)$$

$$v''|_i = \frac{v_{i+1} - 2v_i + v_{i-1}}{h^2},\ \theta''|_i = \frac{\theta_{i+1} - 2\theta_i + \theta_{i-1}}{h^2}$$

$$\phi''|_i = \frac{\phi_{i+1} - 2\phi_i + \phi_{i-1}}{h^2} \qquad (28)$$

the system of ODES $(21)-(24)$ is discretized in space by applying the FDM which is the main step. We substitute from (27) and (28) into $(21)-(24)$ and ignore the truncation errors. Then $(i = 0,1,.....,N)$, the resulting algebraic equations take the form:

$$F_{i+1} - F_{i-1} - 2hV_i = 0 \qquad (29)$$

$$V_{i+1} - 2V_i + V_{i-1} + 0.5h\gamma\left[(V_{i+1} - V_{i-1})(F_i - 0.5S\eta_i)\right.$$
$$\left. - 2h(V_i + S + Da)V_i + 2hM\, F_i\right] = 0 \qquad (30)$$

$$\theta_{i+1} - 2\theta_i + \theta_{i-1} + 0.5h\gamma\,\mathrm{Pr}\, h\left[-1.5hS\theta_i + (\theta_{i+1} - \theta_{i-1})\right.$$
$$\left.(F_i + 0.5S\eta_i) - 2h(F_{i+1} - F_{i-1})\theta_i\right] = 0 \qquad (31)$$

$$\phi_{i+1} - 2\phi_i + \phi_{i-1} + h\gamma\, Sc\left[-1.5hS\phi_i + (\phi_{i+1} - \phi_{i-1})\right.$$
$$\left.(F_i + 0.5S\eta_i) - 2h(F_{i+1} - F_{i-1})\phi_i\right] = 0 \qquad (32)$$

Also, the boundary conditions are

$$F_0 = 1, \theta_0 = 1, \phi_0 = 1, F_N = 0, \theta_N = 0, \phi_N = 0 \qquad (33)$$

The system of equations $(29)-(32)$ is a nonlinear system of algebraic equations F_i, θ_i and ϕ_i. We have solved these equations by applying the Newton iteration method with the help of MATLAB ODE45 software.

5. Results and Discussions

The time-dependent magneto-convective heat-mass transport upon a stretching sheet in a saturated permeable medium has been investigated numerically. The transformed initial value problems (17)–(19) including the boundary conditions (20)–(21) are solved numerically using shooting technique with "ODE45 MATLAB" software. This temperature, velocity, and concentration distributions are displayed in Figs. 2-8 for separate values of the non-dimensional numbers or parameters. The constant values for different parameters or numbers are chosen $\gamma = 16,\ Da = 0.6,\ \mathrm{Pr} = 0.71,\ M = 0.5,\ Sc = 0.5$ and $S = 0.8$.

5.1 Effect of the magnetic force parameter (M) on the velocity profile

Fig. 2 shows the effect of the magnetic force parameter *(M)* on the velocity profile. Increasing values of the magnetic force parameter the fluid velocity decreases. A resistive type of force generates rising values of the magnetic force such as a drag force being created. This drag type of force is said to be Lorentz force. In the computational domain, the Lorentz force obstructs the fluid velocity. So, the fluid would not move freely. Therefore, the velocity of the fluid reduces for growing values of the magnetic force parameter which is a physical phenomenon.

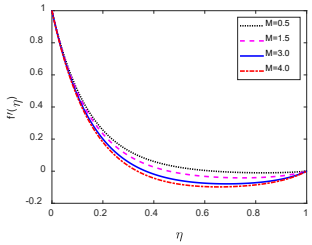

Fig.2 Velocity profile for M

5.2 Effect of the Darcy number (Da) on the velocity, temperature and concentration profiles

Fig. (3-5) demonstrates the effect of the Darcy parameter (Da) on the velocity, temperature, and concentration profiles. It is found from fig.3 that the velocity lessens as the Darcy parameter improves along the plate and the reverse is true away from the plate. It is seen from fig.4 that the fluid temperature increases for increasing values of the Darcy number. Also, it is observed from fig.5 that with uplifting values of the Darcy number the fluid concentration increases. This is because the permeable medium produces a obstruct type of force that reduces fluid velocity and increases fluid temperature and concentration.

5.3 Effect of the Prandtl number (Pr) on the temperature profile

The impact of Prandtl number (Pr) on the temperature distribution is shown in Fig.6. The Prandtl number is inversely proportionate to the thermal conductivity. The thermal conductivity reduces for rising values of the Prandtl number. For this reason, the heat transfer rate improves. Hence, the fluid temperature decrease. The higher Prandtl number has relatively a lower thermal conductivity. It lessens heat conduction and so, the fluid temperature diminishes.

5.4 Effect of the Schmidt number (Sc) on the concentration profile

Fig.7 shows the impact of the Schmidt number (Sc) on the concentration distribution. We know that the Schmidt number is inversely proportional to the molecular (species) diffusivity. From Fig.7 it is seen that for increasing values of *Sc*, the concentration boundary layer becomes thinner. This leads to reducing the concentration profiles. Physically, molecular diffusivity lessens due to improving in the magnitude of *Sc*. For that reason, the species concentration is lower for large values of the Schmidt number and higher for small values of the Schmidt number.

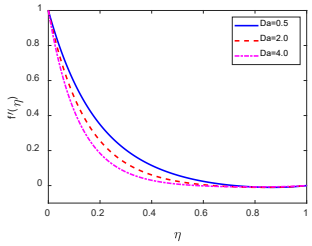

Fig.3 Velocity profile for Da

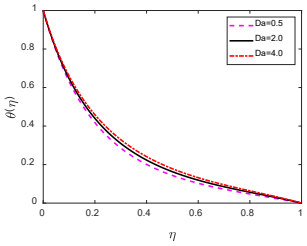

Fig.4 Temperature profile for Da

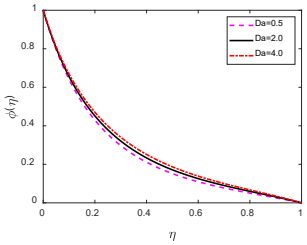

Fig.5 Concentration profile for Da

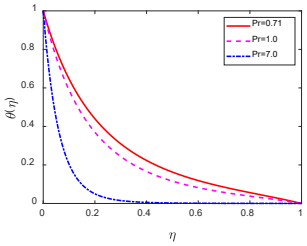

Fig.6 Temperature profile for Pr

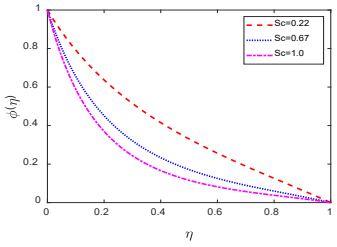

Fig.7 Concentration profile for Sc

5.5 Effect of the unsteadiness parameters (S) on the velocity, temperature and concentration profiles

The impact of the unsteadiness parameter (S) on the velocity, the temperature, and the concentration profiles are shown in Figs. 8, 9, and 10, respectively. It can be concluded from Fig. 8 that the fluid velocity improves for rising values of the unsteadiness parameter *S*. The same behavior can be found for the temperature and concentration profiles when the *S* increases in Fig. 9 and 10.

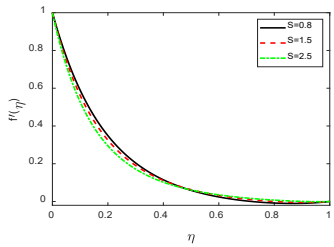

Fig.8 Velocity profile for S

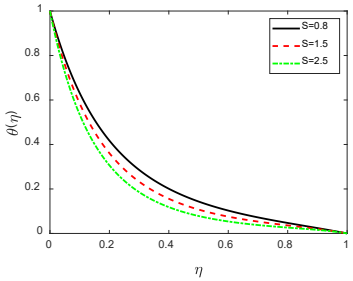

Fig.9 Temperature profile for S

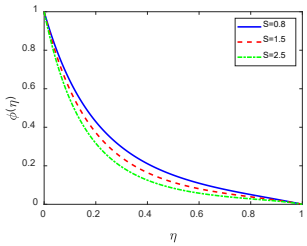

Fig.10 Concentration profile for S

6. Skin friction coefficient, heat and mass transfer rates

Tables 1 to 4 represent the local skin friction coefficient, heat and mass transfer rates for several values of the non-dimensional numbers or parameters It can be seen from Tables 1 and 2 that the local skin friction coefficient increases for rising values of the Darcy number and magnetic force parameter. For this reason, the fluid velocity decreases. From Table 3, it can be concluded that the heat transfer rate increases for moving values of the Prandtl number. Hence, the fluid temperature decrease for rising values of the Prandtl number. With rising values of the Schmidt number, the mass transfer rate enhancement is displayed in Table 4. Therefore the fluid concentration decreases for moving values of the Schmidt number.

Table 1: Effect of Darcy number (Da)

Da	$f''(0)$	$-\theta'(0)$	$-\phi'(0)$
0.5	-5.342	4.867	2.558
2.0	-6.910	4.691	2.460
4.0	-8.577	4.534	2.379

Table 2: Effect of magnetic force parameter (M)

M	$f''(0)$	$-\theta'(0)$	$-\phi'(0)$
0.5	-6.910	4.691	2.460
1.5	-7.048	4.691	2.460
3.0	-7.242	4.691	2.460
4.0	-7.363	4.691	2.460

Table 3: Effect of Prandtl number (Pr)

Pr	$f''(0)$	$-\theta'(0)$	$-\phi'(0)$
0.71	-6.910	4.691	2.460
1.0	-6.910	5.701	2.460
7.0	-6.910	16.681	2.460

Table 4: Impact of Schmidt number (Sc)

Sc	$f''(0)$	$-\theta'(0)$	$-\phi'(0)$
0.22	-6.910	4.691	2.460
0.67	-6.910	4.691	4.538
1.0	-6.910	4.691	5.703

7. Conclusions

The time-dependent magneto-convective heat-mass transport upon a stretching sheet in a saturated permeable medium has been investigated numerically. The following remarks may be drawn:

- The fluid velocity reduces for moving values of the unsteadiness parameter, magnetic force parameter, and Darcy number.
- The temperature of the fluid decreases for increasing values of the Prandtl number.
- Increasing values of the Schmidt number the concentration of fluid diminishes.
- With moving values of the magnetic force parameter (1.5-3.0) and Darcy number (0.6-1.6) the local skin-friction coefficient decreases by about 24% and 21%, respectively.
- The heat transfer rate improves by about 22% for rising values of the Prandtl number (0.71-1.0).
- improving values of the Schmidt number (0.5-1.0) the mass transfer rate improvement by about 46%.

The outcome of this paper may be helpful for geothermal extraction, chemical processing equipment, polymer processing, crystal growing, pollution of groundwater, tinning of copper wires, reactor fluidization, geophysical thermal insulation, welding, etc.

7. References

1. Hasimoto, H. (1957). Boundary layer growth on a flat plate with suction or injection. *Journal of the Physical Society of Japan*, *12*(1), 68-72.
2. Cheng, P. (1977). Combined free and forced convection flow about inclined surfaces in porous media. *Int. J. Heat Mass Transfer, 20*, 807-814.
3. Sharma, G. K., Kumar, L. K., & Singh, N. K. (2016). Unsteady flow through porous media past on moving vertical plate with variable temperature in the presence of inclined magnetic field. *International journal of innovative technology and research (ijtr) Vol. No. 4, Issue No*, *2*, 2784-2788.
4. Gupta, P. S., & Gupta, A. S. (1977). Heat and mass transfer on a stretching sheet with suction or blowing. *The Canadian journal of chemical engineering*, *55*(6), 744-746.
5. Noor, N. F. M., & Hashim, I. (2010). Thermocapillarity and magnetic field effects in a thin liquid film on an unsteady stretching surface. *International Journal of Heat and Mass Transfer*, *53*(9-10), 2044-2051.
6. Wang, C., & Pop, I. (2006). Analysis of the flow of a power-law fluid film on an unsteady stretching surface by means of homotopy analysis method. *Journal of Non-Newtonian Fluid Mechanics*, *138*(2-3), 161-172.
7. Khader, M. M., & Megahed, A. M. (2013). Numerical simulation using the finite difference method for the flow and heat transfer in a thin liquid film over an unsteady stretching sheet in a saturated porous medium in the presence of thermal radiation. *Journal of King Saud University-Engineering Sciences*, *25*(1), 29-34.
8. Hasanuzzaman, M., Afroj, R., Sharin, S., & Miyara, A. (2022). Thermal Radiation Effect on Unsteady Convection and Mass Transport Over a Stretching Sheet in a Saturated Porous Medium With Chemical Reaction, Scientific Reports, and Research Square (submitted).
9. Ali, J. C., Sameh, E. A., & Abdulkareem, S. A. (2010). Melting and radiation effects on mixed convection from a vertical surface embedded in a non-Newtonian fluid saturated non-Darcy porous medium for aiding and opposing eternal flows. *International Journal of Physical Sciences*, *5*(7), 1212-1224.
10. Cheng, W. T., & Lin, C. H. (2008). Unsteady mass transfer in mixed convective heat flow from a vertical plate embedded in a liquid-saturated porous medium with melting effect. *International Communications in Heat and Mass Transfer*, *35*(10), 1350-1354.

NOMENCLATURE

u	velocity component along the x-axis
v	velocity component along the y-axis
T	temperature of fluid
C	fluid concentration
T_s	surface temperature
C_s	surface concentration
T_{ref}	reference temperature
C_{ref}	reference concentration
T_0	temperature at the slit
C_0	concentration at the slit
$U(x,t)$	uniform surface velocity
$h(t)$	thin liquid film thickness
α	thermal diffusivity
β	fluid density
μ	dynamic viscosity
υ	kinematic viscosity
K	permeability of surface
$D*$	coefficient of mass diffusion
C_p	specific heat at constant pressure
η	similarity variable
$f'(\eta)$	dimensionless velocity
$\theta(\eta)$	dimensionless temperature
$\phi(\eta)$	dimensionless concentration
Sc	Schmidt number
Pr	Prandtl number
M	Magnetic force parameter
k	thermal conductivity
t	time
Da	Darcy number
C_f	local skin-friction coefficient
Nu_x	local Nusselt number
Sh_x	local Sherwood number
Re_x	local Reynolds number
$f''(0)$	local skin friction coefficient
$\theta'(0)$	heat transfer rate
$\phi'(0)$	mass transfer rate